Contribution from Salutar, Inc., 428 Oakmead Parkway, Sunnyvale, California 94086, and the Department of Chemistry, University of California, Berkeley, California 94720

Structural and Thermodynamic Characterization of Manganese(II) *N,N'*-Dipyridoxylethylenediamine-*N,N'*-diacetate. A Novel Manganese(II) Chelate

Scott M. Rocklage,*[1] Steven H. Sheffer,[1] William P. Cacheris,[1] Steven C. Quay,[1] F. Ekkehardt Hahn,[2] and Kenneth N. Raymond[2]

Received February 29, 1988

The crystal structure and solution equilibrium properties of manganese(II) *N,N'*-dipyridoxylethylenediamine-*N,N'*-diacetate, Mn(PLED^{2-}), have been determined. The molecule has a 2-fold axis passing through the manganese atom and the C11-C11' ethylenediamine backbone. Crystals of $MnC_{22}H_{28}N_4O_8 \cdot 4H_2O$ are monoclinic, space group $C2/c$ (No. 15), with a = 20.388 (2) Å, b = 9.0769 (12) Å, c = 14.3588 (15) Å, β = 98.968 (8)°, and Z = 4. The manganese(II) oxidation state was confirmed by Mn-O1, Mn-O2, and Mn-N2 bond distances and by magnetic susceptibility measurements. The thermodynamic stability constants for Mn(II), Zn(II), and Cu(II) were determined potentiometrically. log K_{ML} was determined to be 12.56, 16.68, and 21.52 for Mn(PLED^{2-}), Zn(PLED^{2-}), and Cu(PLED^{2-}), respectively.

Introduction

Taliaferro et al.[3] have reported the solution equilibria properties of the ligand *N,N'*-dipyridoxylethylenediamine-*N,N'*-diacetic acid, PLED, with a wide variety of metal ions. In general, the stability constants for PLED metal chelates were 2-3 orders of magnitude less than those found for chelates derived from HBED, *N,N'*-bis(hydroxybenzyl)ethylenediamine-*N,N'*-diacetic acid, or EHPG, *N,N'*-ethylenebis[2-(*o*-hydroxyphenyl)glycine]. All three ligands contain six donor groups (two ethylenediamine nitrogens, two carboxylates, and two phenolates) that are available for metal binding. The different ligand basicities, geometries, and steric effects play important roles in determining the overall stabilities of the various chelates of PLED, HBED, and EHPG. While EHPG contains two carboxylate groups on the benzyl carbon atoms, HBED and PLED contain acetate groups on the ethylenediamine nitrogen atoms. In addition, PLED contains pyridoxal rings with sterically demanding methyl groups. The diminished basicities of the PLED phenolates and aliphatic nitrogens contribute to the reduced thermodynamic stability of its complexes relative to those of EHPG and HBED.[3a]

In this paper we report the complexation chemistry of PLED with manganese(II). Relatively few manganese(II) coordination compounds are known, and only a small number of these have been completely characterized, including those studied by X-ray diffraction.[4-7] Attempts to prepare manganese(II) complexes of EHPG and HBED resulted in rapid oxidation and hydrolysis at neutral pH.

Most of the structurally characterized Mn(II) complexes have various mono- and bidentate ligands coordinating to the metal center. Mn(PLED^{2-})·4H$_2$O (**1**) represents the first structurally characterized Mn(II) complex with a high-affinity hexadentate ligand. Complexes of the paramagnetic high-spin manganese(II) ion, particularly hydrolytically stable ones, are of interest as magnetic resonance imaging (MRI) enhancement agents.[8-11]

In addition, radiopharmaceutical applications of PLED with ^{68}Ga and ^{111}In have been recently investigated.[12] The radiolabeled complexes did not cross the intact blood-brain barrier or exhibit specificity for any organ other than the kidney.

The synthesis, isolation, solution equilibria, and crystal structure of Mn(PLED^{2-})·4H$_2$O are reported. We also investigated the solution equilibria of two other biologically occurring metal(II) ions with PLED, copper and zinc.

Experimental Section

Ligand Synthesis. The ligand PLED·2H$_2$O was synthesized by modification of the procedure of Taliaferro et al.[3a]

Synthesis of *N,N'*-Dipyridoxylethylenediamine. Ethylenediamine (6 g, 0.1 mol) and sodium hydroxide (8 g, 0.2 mol) were dissolved in deionized water (8 mL) and methanol (250 mL). While the mixture was stirred, a fine powder of pyridoxal hydrochloride (40.7 g, 0.2 mol) was added, and the resulting yellow suspension of the Schiff base was stirred for 1 h. After addition of diethyl ether (100 mL) and stirring for 5-10 min, the suspension was filtered and the intermediate imine collected. The damp imine was stirred in ethanol (400 mL), and NaBH$_4$ (9 g, 0.24 mol) was added in small portions. Discharge of the yellow imine color occurred as the reduction progressed. After final addition of NaBH$_4$, the solution was stirred for 1 h and the crude product isolated by filtration. Additional product can be recovered from the filtrate. The product was then dissolved in 1 N NaOH (200 mL) and filtered if necessary, followed by adjustment to pH 9.8 with 6 N HCl. The amine precipitated in the refrigerator and was isolated by filtration, washed with cold water, and dried in vacuo to yield 30.8 g (85%). ^{1}H NMR in D$_2$O/NaOD (Bruker AM250; ppm from TMS): 6.98 (s, 2 H, py *H*), 3.97 (s, 4 H, C*H*$_2$OH), 3.25 (s, 4 H, NC*H*$_2$-py), 2.13 (s, 4 H, NC*H*$_2$C*H*$_2$N), 1.82 (s, 6 H, py-C*H*$_3$).

Synthesis of *N,N'*-Dipyridoxylethylenediamine-*N,N'*-diacetic Acid. The diamine product from above was placed in a 2-L four-neck flask containing deionized water (100 mL), and the reaction flask was positioned in a warm water bath. The flask was then fitted with a pH electrode and thermometer. Separate addition funnels containing a 40-mL solution of NaOH (20 g, 0.5 mol) and a 30-mL solution of BrCH$_2$COOH (24 g, 0.17 mol) were positioned in the remaining two necks of the flask. A 20-mL portion of the NaOH solution was added to the reaction mixture while it was being stirred, and the amine dissolved, yielding a yellow solution (pH 12). The reaction mixture was heated until the solution reached 40 °C. BrCH$_2$COOH was added rapidly until the pH dropped to 11.0. Simultaneously, the BrCH$_2$COOH and NaOH solutions were slowly added so that the solution was maintained at pH 11.1 ± 0.1. After final addition of the BrCH$_2$COOH solution, the reaction mixture was stirred for 1 h, and IRC-50 (~200 g) ion-exchange resin was added to lower the pH to 6.1. After the resin was filtered out and washed with water (100 mL), the filtrate was stirred while IR-120 (30 g) ion-exchange resin was added until the pH dropped to 3.5. The IR-120 resin was filtered out, and the filtrate was concentrated to 60 mL and transferred to a 1-L beaker. The product was crystallized by addition of CH$_3$OH (~500 mL) with stirring, followed by refrigeration overnight. Addition of CH$_3$CH$_2$OH (250 mL) precipitated more product, which was

(1) Salutar, Inc.
(2) University of California.
(3) (a) Taliaferro, C. H.; Motekaitis, R. J.; Martell, A. E. *Inorg. Chem.* **1984**, *23*, 1188. (b) Taliaferro, C. H.; Martell, A. E. *Inorg. Chem.* **1985**, *24*, 2408-2413.
(4) Neupert-Laves, K.; Dobler, M. *Helv. Chim. Acta* **1977**, *60*, 1861-1871.
(5) Gott, G. A.; Fawcett, J.; McAuliffe, C. A.; Russell, D. R. *J. Chem. Soc., Chem. Commun.* **1984**, 1283-1284.
(6) Garrett, T. P.; Mitchell, G.; Freeman, H. C. *Acta Crystallogr., Sect. C: Cryst. Struct. Commun.* **1983**, *C39*, 1027-1031, 1031-1034.
(7) Mabad, B.; Cassoux, P.; Tuchagues, J.-P.; Hendrickson, D. N. *Inorg. Chem.* **1986**, *25*, 1420-1431.
(8) Koenig, S. H.; Baglin, C.; Brown, R. D., III; Brewer, C. F. *Magn. Reson. Med.* **1984**, *1*, 496-501.
(9) Koenig, S. H.; Brown, R. D., III. *J. Magn. Reson.* **1985**, *61*, 426-439.
(10) Jackels, S. C.; Kroos, B. R.; Hinson, W. H.; Karstaedt, N.; Moran, P. R. *Radiology* **1986**, *159*, 525-530.
(11) Lyon, R. C.; Faustino, P. J.; Cohen, J. S.; Katz, A.; Mornex, F.; Colcher, D.; Baglin, C.; Koenig, S. H.; Hambright, P. *Magn. Reson. Med.* **1987**, *4*, 24-33.
(12) Green, M. A.; Welch, M. J.; Mathias, C. J.; Taylor, P.; Martell, A. E. *Int. J. Nucl. Med. Biol.* **1985**, *12*, 381-386.

0020-1669/88/1327-3530$01.50/0

Table I. Crystallographic Data for Mn(PLED^{2-})·4H_2O

$MnC_{22}H_{28}N_4O_8 \cdot 4H_2O$	space group $C2/c$ (No. 15)
a = 20.388 (2) Å	T = 25 °C
b = 9.0769 (12) Å	λ (Mo Kα) = 0.710 73 Å
c = 14.3588 (15) Å	μ = 5.49 cm^{-1}
β = 98.968 (8)°	transmission coeff = 0.97–0.98
V = 2624.7 Å^3	$R(F_o)$ = 3.19%
Z = 4	$R_w(F_o)$ = 5.18%
mol mass 603.49 amu	

allowed to stand at 5 °C for 4 h before filtering. The product was dried in vacuo to yield 15.5 g. A second recrystallization was performed by dissolving the product in boiling water (30 mL) in a 500-mL beaker and adding MeOH (300 mL). The rapidly solidifying mixture was refrigerated overnight. The solid was filtered out and dried in vacuo to yield 11.5 g of pure product (22%). ^{1}H NMR in D_2O/NaOD (Bruker AM20, ppm from TMS): 7.73 (s, 2 H, py *H*), 4.54 (s, 4 H, CH_2OH), 4.12 (s, 4 H, NCH_2-py), 3.27 (s, 4 H, CH_2COOH), 2.98 (s, 4 H, NCH_2CH_2N), 2.30 (s, 6 H, py-CH_3). Anal. Calcd for $C_{22}H_{30}N_4O_8 \cdot 2H_2O$: C, 51.35; H, 6.66; N, 10.89. Found: C, 51.66; H, 6.67; N, 10.93.

Mn(PLED^{2-})·4H_2O (1). A 50 mM neutral aqueous solution of Mn(PLED)·4H_2O was prepared from $MnCl_2 \cdot 4H_2O$, PLED·2H_2O, and NaOH. The yellow-orange solution is slightly air and light sensitive and slowly darkens with exposure. X-ray-quality yellow-orange crystals of **1** can be obtained from a concentrated solution left standing at room temperature. The crystals lose water of crystallization in dry air (hence the formula given below differs from that of the single crystal). Anal. Calcd for $C_{22}H_{28}N_4O_8Mn \cdot 1.5H_2O$: C, 47.31; H, 5.55; N, 10.03. Found: C, 47.36; H, 5.48; N, 9.83.

X-ray Data Collection of 1. A suitable crystal was placed in a thin-walled glass capillary. Preliminary X-ray examination of the crystal on a precession camera indicated the symmetry of the crystal lattice (monoclinic) and yielded the preliminary dimensions of the unit cell. The crystal was transferred to an Enraf-Nonius CAD-4 diffractometer for data collection.[13] Final cell parameters were obtained by least squares from the angular setings of 24 strong reflections well spaced throughout reciprocal space in the 2θ range 27.08° ≤ 2θ ≤ 31.50°. With the use of θ–2θ scan techniques and Mo Kα radiation, all intensity data (h,k,±l) were collected at 25 °C in the 2θ range 2° ≤ 2θ ≤ 45°. A total of 3285 intensity data were collected. The intensities of three standard reflections, (3,−1,9), (−1,−5,−5), and (2,−6,−3) were measured every 2 h of X-ray exposure time. Three orientation control reflections were remeasured after every 200 intensity measurements. A new orientation matrix was calculated from an array of 24 reflections if any of the orientation standards was offset from its predicted position by more than 0.1°. Reorientation was necessary twice during data collection. Azimuthal scans were recorded for six reflections near χ = 90° at 10° increments of rotation of the crystal about the diffraction vector. Final crystal and data collection details are summarized in Tables I and SI (supplementary material).[14]

Structure Solution and Refinement of 1. The raw intensity data were converted to structure factor amplitudes (and their esd's) by correction for scan speed, background, and Lorentz and polarization effects.[15] Inspection of the list of intensity standards of reflections revealed that no correction for crystal decomposition was necessary. The azimuthal scan data showed a variation of ±3%; hence, no correction for absorption was applied.

Systematically absent reflections (hkl, $h + k = 2n + 1$; $h0l$, $l = 2n + 1$), all reflections $0kl$, $l < 0$, and 36 strong reflections that were not measured accurately were removed from the data set, leaving 1672 unique data. From the systematic absent reflections, the space group was determined to be either Cc (No. 9) or $C2/c$ (No. 15). Solution and refinement of the structure was achieved in the centric space group $C2/c$ with Z = 4.

The structure was solved by standard heavy-atom techniques. The atomic positional parameters were refined in stages by using first isotropic and later anisotropic thermal parameters. A subsequent difference Fourier map revealed the positional parameters of all hydrogen atoms. Hydrogen atoms HN1, HW1–HW4, and HO2 were added to the structure model at the positions obtained from the difference Fourier map with a constant isotropic thermal parameter of B_{eq} = 4.0 Å^2. All other

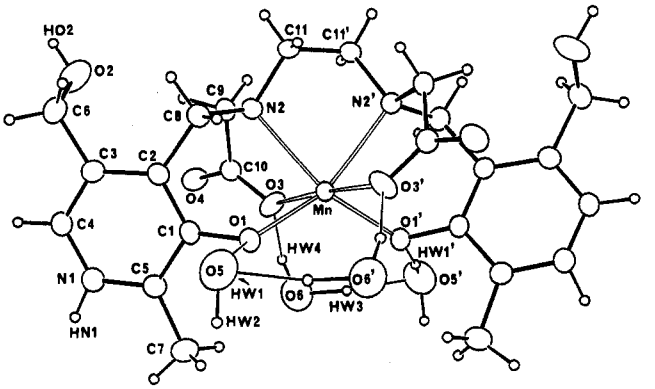

Figure 1. ORTEP[24] drawing of one molecule of Mn(PLED^{2-})·4H_2O with the employed atom-numbering scheme. Ellipsoids in Figures 1 and 2 are scaled to represent the 50% probability surface. Hydrogen atoms were given orbital radii. The asymmetric unit contains half of the molecule and two water molecules. Mn occupies a special position on the 2-fold axis, which also passes through the midpoint of the C11–C11′ bond. The three intramolecular hydrogen bonds (Table IV) are indicated by thin lines. HW1 is hidden behind O5.

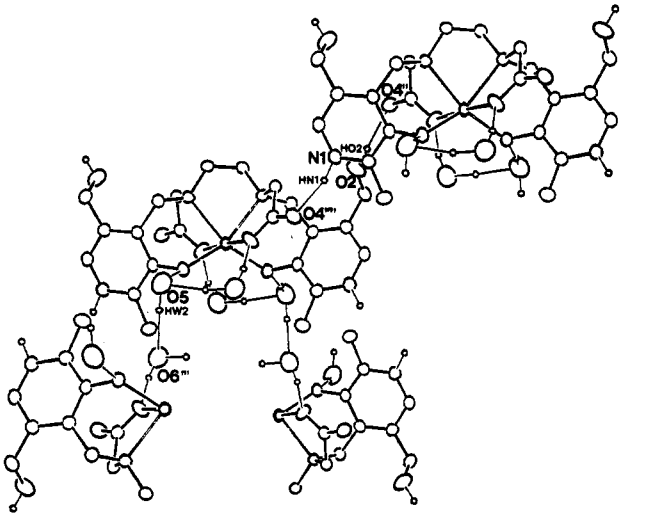

Figure 2. Intramolecular and intermolecular hydrogen bonds in **1**. Only atoms involved in intermolecular hydrogen bonds (Table IV) are labeled.

hydrogen atoms were introduced at calculated positions (d(C–H) = 0.95 Å, d(N–H) = 0.87 Å)[16] with isotropic thermal parameters 1.3 times larger than the B_{eq} of the atom to which they are bonded. No hydrogen atom parameters were refined. A test for secondary extinction was negative.

The quantity minimized by the least-squares program was $\sum w(|F_o| - |F_c|)^2$, where w is the weight of a given observation.[13] Atomic scattering factors for the neutral atoms were used,[17] and all non-hydrogen scattering factors were corrected for both the real and the imaginary components of anomalous dispersion.[18] Inspection of the residuals ordered in ranges of (sin θ)/λ, $|F_o|$, and parity and value for the individual index showed no unusual features or trends. The largest positive peak in the final difference Fourier map had an electron density of 0.30 e/Å^3 and was located 0.78 Å from atom N1. The largest negative peak in this map had an intensity of 0.23 e/Å^3. The final residuals for 177 variables refined against 1580 data with $F_o \geq 3\sigma(F_o^2)$ were R = 3.19%, R_w = 5.18%, and GOF = 3.099. The R value of all 1672 unique data is 3.54%.

Final positional and thermal parameters for all atoms are listed in Table II. The atomic numbering scheme followed in these listings is identified in Figures 1 and 2. Table III lists intramolecular bond distances and angles. Selected parameters of intramolecular and intermolecular hydrogen bonds are given in Table IV.[14]

Potentiometric Measurements. All potentiometric measurements on PLED were made with an automatic titrator system. The system con-

(13) A detailed outline of the data collection and reduction procedures can be found in: Eigenbrot, C. W.; Raymond, K. N. *Inorg. Chem.* **1982**, *21*, 2650–2653.
(14) See paragraph at the end of this paper for available supplementary material.
(15) *SDP User's Guide*; B. A. Frenz & Associates: College Station, TX, 1982.
(16) Churchill, M. R. *Inorg. Chem.* **1973**, *12*, 1213.
(17) Cromer, D. T.; Waber, J. T. *International Tables for X-Ray Crystallography*; Kynoch: Birmingham, England, 1974; Vol. IV, Table 2.2B.
(18) Reference 17, Table 2.3.1.

Table II. Positional Parameters and Isotropic Equivalent Thermal Parameters for $Mn(PLED^{2-})\cdot 4H_2O$

atom	x	y	z	B, Å²[a]	atom	x	y	z	B, Å²[a]
Mn[b]	0.000	0.13732 (4)	0.250	1.611 (8)	C11	0.02735 (9)	−0.1934 (2)	0.2923 (1)	2.01 (4)
O1	0.06700 (6)	0.2533 (2)	0.34846 (9)	2.15 (3)	HN1	0.2343	−0.0839	0.1464	4.0*
O2	0.25934 (9)	−0.1659 (2)	0.3509 (1)	3.64 (4)	HW1	0.0664	0.3046	0.4785	4.0*
O3	0.07670 (8)	0.1455 (1)	0.1538 (1)	2.49 (3)	HW2	0.0664	0.4433	0.5410	4.0*
O4	0.17419 (7)	0.0625 (2)	0.1236 (1)	2.46 (3)	HO2	0.2832	−0.2500	0.3535	4.0*
O5	0.06338 (9)	0.3336 (2)	0.5376 (1)	4.15 (4)	HW3	0.0156	0.3612	0.0195	4.0*
O6	0.0760 (1)	0.3630 (2)	0.0174 (2)	4.71 (5)	HW4	0.0840	0.2773	0.0625	4.0*
N1	0.23978 (8)	0.3241 (2)	0.3693 (1)	1.93 (3)	H4	0.3141	0.1828	0.4079	2.5*
N2	0.07076 (7)	−0.0653 (2)	0.2895 (1)	1.66 (3)	H61	0.3065	−0.0546	0.4560	3.0*
C1	0.13090 (9)	0.2285 (2)	0.3596 (1)	1.73 (4)	H62	0.2395	−0.1191	0.4755	3.0*
C2	0.15862 (9)	0.0878 (2)	0.3818 (1)	1.65 (4)	H71	0.1860	0.5600	0.3194	3.8*
C3	0.2278 (1)	0.0714 (2)	0.4006 (1)	1.79 (4)	H72	0.1237	0.4902	0.2600	3.8*
C4	0.2672 (1)	0.1922 (2)	0.3944 (1)	1.89 (4)	H73	0.1228	0.5323	0.3645	3.8*
C5	0.1743 (1)	0.3470 (2)	0.3509 (1)	1.86 (4)	H81	0.1361	−0.1258	0.4034	2.5*
C6	0.2616 (1)	−0.0728 (2)	0.4298 (1)	2.29 (4)	H82	0.0824	−0.0182	0.4285	2.5*
C7	0.1495 (1)	0.4958 (2)	0.3211 (2)	2.95 (5)	H91	0.0974	−0.1617	0.1758	2.4*
C8	0.1114 (1)	−0.0395 (2)	0.3844 (1)	1.91 (4)	H92	0.1578	−0.1145	0.2493	2.4*
C9	0.1152 (1)	−0.0859 (2)	0.2180 (1)	1.85 (4)	H111	0.0077	−0.1898	0.3480	2.6*
C10	0.1227 (1)	0.0518 (2)	0.1618 (1)	1.85 (4)	H112	0.0528	−0.2809	0.2921	2.6*

[a] Starred values indicate atoms were included with isotropic thermal parameters and are unrefined. The thermal parameter given for anisotropically refined atoms is the isotropic equivalent thermal parameter defined as $(4/3)[a^2B(1,1) + b^2B(2,2) + c^2B(3,3) + ab(\cos\gamma)B(1,2) + ac(\cos\beta)B(1,3) + bc(\cos\alpha)B(2,3)]$, where a, b, and c are real cell parameters. [b] Mn occupies a special position on the 2-fold axis (Wyckoff position e); its positional parameters were fixed to $x = 0.0$ and $z = 0.25$.

Table III. Intramolecular Distances (Å) and Angles (deg) for $Mn(PLED^{2-})\cdot 4H_2O$

		Distances	
Mn–O1	2.0907 (8)	N2–C9	1.484 (2)
Mn–O3	2.2434 (9)	N2–C11	1.4658 (15)
Mn–N2	2.3513 (10)	C1–C2	1.413 (2)
O1–C1	1.3072 (14)	C1–C5	1.411 (2)
O2–C6	1.408 (2)	C2–C3	1.401 (2)
O3–C10	1.2576 (15)	C2–C8	1.508 (2)
O4–C10	1.2618 (15)	C3–C6	1.508 (2)
N1–C4	1.347 (2)	C5–C7	1.482 (2)
N1–C5	1.336 (2)	C11–C11′[a]	1.515 (3)
N2–C8	1.4985 (15)		
		Angles	
O1–Mn–O3	87.42 (3)	O1–C1–C2	122.66 (11)
O1–Mn–N2	85.36 (3)	O1–C1–C5	118.97 (11)
O1–Mn–O1′[a]	119.52 (5)	C1–C2–C3	119.63 (11)
O1–Mn–O3′	90.67 (3)	C1–C2–C8	117.61 (10)
O1–Mn–N2′	150.29 (3)	C2–C3–C4	119.05 (11)
O3–Mn–N2	73.39 (3)	C2–C3–C6	123.25 (11)
O3–Mn–O3′	176.20 (4)	N1–C4–C3	120.34 (11)
O3–Mn–N2′	109.74 (3)	N1–C5–C1	118.99 (11)
N2–Mn–N2′	77.11 (5)	N1–C5–C7	119.00 (11)
Mn–O1–C1	121.97 (7)	C1–C5–C7	122.0 (12)
Mn–O3–C10	120.18 (7)	O2–C6–C3	109.92 (10)
C4–N1–C5	123.48 (10)	N2–C8–C2	111.22 (9)
Mn–N2–C8	109.18 (7)	N2–C9–C10	112.89 (10)
Mn–N2–C9	110.50 (7)	O3–C10–O4	124.58 (11)
Mn–N2–C11	106.07 (7)	O3–C10–C9	118.25 (11)
C8–N2–C9	109.76 (9)	O4–C10–C9	117.13 (11)
C8–N2–C11	110.48 (9)	N2–C11–C11′	110.52 (8)
C9–N2–C11	110.79 (9)		

[a] Primed atoms represent transformed coordinates of the type $-x$, y, $^1/_2 - z$. Mn lies on a special position on the 2-fold axis, which also passes through the midpoint of the C11–C11′ bond.

sisted of a Model 925 Fisher digital pH meter, a Corning glass and AgCl reference combination electrode, a Model 665 Metrohm digital autoburet, and an IBM-compatible computer. The temperature was maintained at 25.0 ± 0.1 °C with a Lauda RM6 circulating constant-temperature bath connected to a Brinkman 50-mL jacketed titration vessel. The titration vessel was covered with a Brinkman five-hole cap, which held the electrode, buret, and nitrogen inlet. During each titration, oxygen-free nitrogen gas, saturated with CO_2-free deionized water, was slowly blown into the titration vessel (with the remaining two holes stoppered) to exclude the atmosphere. The pH meter was standardized with pH 2.00, 4.000, 7.000, 10.000, and 12.00 buffer solutions (± 0.02, 0.002, 0.002, 0.002, and 0.02, respectively) to read hydrogen activity, and the readings were found to be linear over this pH range. The value for the hydrogen ion activity coefficient was determined by measuring hydrogen ion activity for standard HCl solutions at an ionic strength of 0.10 M (NaCl). The value found for hydrogen ion activity at 0.10 M (NaCl) was 0.782. The value for pK_w was found to be 13.79.

Table IV. Intramolecular and Intermolecular Hydrogen-Bond Parameters (Å, deg) for $Mn(PLED^{2-})\cdot 4H_2O$[a]

A–H···B	H···B dist	∠A–H–B	A–B dist
	Intramolecular Parameters		
O5–HW1···O1	1.93	175.4	2.8238 (14)
O6–HW4···O3	1.80	163.3	2.7794 (13)
O6–HW3···O5′	1.71	149.1	2.841 (2)
	Intermolecular Parameters		
O2–HO2···O4″	1.92	170.1	2.8097 (13)
O5–HW2···O6‴	1.81	165.6	2.786 (2)
N1–HN1···O4″	1.80	155.9	2.7769 (13)

[a] All hydrogen positions are unrefined. Symmetry codes for primed atoms are as follows: (single prime) $-x$, y, $^1/_2 - z$; (double prime) $^1/_2 - x$, $-^1/_2 + y$, $^1/_2 - z$; (triple prime) x, $1 - y$, $^1/_2 + z$.

All solutions were prepared at ionic strength 0.10 M (NaCl) with deionized water that was boiled and purged with N_2 while cooling to ensure removal of CO_2. Stock solutions of the metal ions were made from the metal chlorides in CO_2-free deionized water and were standardized by titration with EDTA.[19] The sample solution was prepared by dissolving solid PLED·$2H_2O$ ($C_{22}H_{30}N_4O_8\cdot 2H_2O$, >99.5% pure by titration[20]) in CO_2-free deionized water in a volumetric flask along with the required amount of metal salt stock solution so that the metal:ligand ratio was 1:1 (between 3×10^{-3} and 5×10^{-3} M). In the competitive titrations, solid PLED·$2H_2O$ and solid H_4EDTA (99% pure, Sigma Chemical Co.) were dissolved in a volumetric flask along with metal stock solution so that the Cu^{2+}:PLED:EDTA ratios were 1:1:1. In each sample solution a small amount of CO_2-free 5 N NaOH (J. T. Baker) was then added so that the pH of sample solution was approximately 11 before dilution to volume. All sample solutions showed no visible indications of metal hydroxide precipitation at pH 11. An aliquot of the sample solution was placed in the titration vessel and titrated with CO_2-free 0.10000 M HCl to minimize ionic strength changes during the course of the titration. For each system, four titrations were performed and reproducible results were obtained. The eds's are reported in parentheses in Table V.

Automatic titration control was accomplished by an in-house BASIC program that utilizes windowing to simultaneously display a high-resolution plot of the titration along with a tabular display of the accumulated data. After each addition of titrant, the solution was stirred for 15 s, after which nine pH readings were taken at 2-s intervals. If the highest and

(19) *Reagent Chemicals*, 6th ed.; American Chemical Society: Washington, DC, 1985; p 217.
(20) Bassett, J.; Denney, R. C.; Jeffrey, G. H.; Mendham, J. *Vogel's Textbook Of Quantitative Inorganic Analysis*; Longman: Birmingham, AL, 1978; p 330.

Table V. Protonation Constants and Metal Chelate Stability Constants of PLED (T = 25 °C, μ = 0.10 M (NaCl))

equilibrium	log K^a	log K^b
[HL]/[L][H]	10.75 (3)	11.10
[H_2L]/[HL][H]	10.33 (13)	10.68
[H_3L]/[H_2L][H]	7.12 (7)	9.54
[H_4L]/[H_3L][H]	5.64 (3)	7.21
[H_5L]/[H_4L][H]	3.12 (9)	5.73[c]
[H_6L]/[H_5L][H]	1.74 (12)	3.31
[H_7L]/[H_6L][H]		2.57
[ZnL]/[Zn][L]	16.68 (15)	16.61
[ZnHL]/[ZnL][H]	8.76 (3)	8.85
[ZnH_2L]/[ZnHL][H]	7.93 (9)	8.22
[CuL]/[Cu][L]	21.52 (5)	19.91
[CuHL]/[CuL][H]	8.70 (11)	8.81
[CuH_2L]/[CuHL][H]	7.75 (8)	7.98
[MnL]/[Mn][L]	12.56 (14)	
[MnHL]/[MnL][H]	8.74 (2)	
[MnH_2L]/[MnHL][H]	7.90 (16)	

[a] This work. [b] Reference 3a. [c] Omitted in ref 3b.

lowest of the nine pH values did not differ by more than 0.005 pH unit, then the readings were averaged for a final value for the data point. If the nine readings varied by more than 0.005 unit, then a new set of nine readings were taken. This procedure was repeated until the pH of the solution dropped below pH 2, which usually yielded 250 data points per titration. This titration scheme provided sufficient time for equilibrium to be reached after each addition of titrant in both direct and competitive ligand titrations.

Stability constants for Mn(PLED^{2-}) and Zn(PLED^{2-}), as well as the protonated forms of the complexes, were determined by direct titration. The stability constant (K_{101}) for Cu(PLED^{2-}), however, could not be accurately determined by direct titration since the complex does not appreciably dissociate at pH 2. Previous workers have determined a stability constant for Cu(PLED^{2-}) of log K_{101} = 19.91.[3a] It can be easily shown that the complex is only ca. 2% dissociated at pH 2. Thus, in this work, the Cu(PLED^{2-}) stability constant was determined by using a ligand–ligand competition titration. The ligand–ligand competition titration experiment involves titrating a 1:1:1 molar ratio mixture of metal ion, PLED, and reference ligand that forms a complex with the metal ion of accurately known stability. It is also essential that the reference ligand be chosen such that during the course of the titration the metal ion significantly transfers between the two ligands. In addition, hydrogen ion is either consumed or liberated during the transfer. For Cu(PLED^{2-}), EDTA was found to be an excellent reference ligand.

Computations. PLED proton association constants were calculated by a BASIC computer program written for polyprotic weak acid equilibrium calculations. The stability constants of the metal ion complexes in both direct titrations and competitive titrations were calculated by a BASIC program designed for a variety of metal ion–ligand–proton systems. Both programs utilize a combined Simplex/Marquardt algorithm for evaluation of the equilibrium constants. A modified Newton–Raphson algorithm[21] is used to calculate −log [H^+] for each data point that is compared to the observed value. In all titrations the average deviation between calculated and observed −log [H^+] was in the range 0.01–0.02.

Magnetic Measurements. The spin-only magnetic moment of Mn(PLED^{2-}) was determined by using a modified version of the NMR method described by Evans.[22] The samples were prepared in D_2O with 2% acetone at pD 6.5. A Mn(PLED^{2-}) concentration of 31.05 mM provided a 484-Hz difference between the acetone resonances in the inner and outer NMR tubes. The $^3/_{2\pi}$ shape factor in the original method is only applicable to electromagnets, and a $^3/_{4\pi}$ shape factor is required for superconducting magnets when concentric NMR tubes are used.

Results and Discussion

Description and Discussion of the Structure. The crystal structure shows the complex consists of discrete molecules of Mn(PLED^{2-}). The Mn(PLED^{2-}) and four water molecules form an infinite polymeric network of hydrogen bonds (Figure 2). The manganese atom lies on a 2-fold axis that passes through the midpoint of the C11–C11′ bond (Figure 1). Thus, the asymmetric unit contains a half molecule of Mn(PLED^{2-}) and two water molecules, with Z = 4 for the unit cell.

The metal coordination site is a distorted octahedron made up by two phenolic oxygen atoms (O1, O1′), two carboxylic oxygen atoms (O3, O3′), and two tertiary nitrogen atoms (N2, N2′), as illustrated in Figure 1. All four coordinating oxygen atoms are negatively charged. Since the two nitrogen atoms of the aromatic ring (N1, N1′) are protonated (HN1 was found in a difference Fourier map), the total charge of the ligand is −2. The ion stoichiometry of the unit cell is thus consistent with the assigned manganese oxidation state of +2. The Mn–O and Mn–N bond distances are also typical for Mn(II). The ionic radius of hexacoordinated manganese decreases with increasing charge on the metal atom: high spin, $r_{Mn^{2+}}$ = 0.830 Å; high spin, $r_{Mn^{3+}}$ = 0.645 Å and $r_{O^{2-}}$ = 1.35 Å.[23] Thus, one would expect a Mn^{2+}–O distance of 2.180 Å and Mn^{3+}–O distances not longer than 1.995 Å. Both Mn–O separations in **1** (Mn–O1 = 2.0907 (8) Å, Mn–O3 = 2.2434 (9) Å) are longer than expected for Mn^{3+} and fall well within the range predicted for Mn^{2+} from ionic radii. Furthermore, the observed Mn–O separations in **1** are in good agreement with some comparable complexes: Mn–O(amide) = 2.19 Å,[4] Mn–O(SO_2) = 2.282 (4) Å,[5] Mn–O(O–P($Ph)_3$) = 2.084 (3) and 2.147 (3) Å.[5] As expected, the Mn–O1 distance in Mn(PLED^{2-}) is shorter than the Mn–O3 distance, due to the greater extent of charge distribution in the carboxylic acid system. The +2 oxidation state is also confirmed by comparison of the Mn–N2 distance to Mn–N distances for divalent manganese[6] and by observation of a spin-only magnetic moment of 5.95 μ_B for Mn(PLED^{2-}) via NMR measurements (the theoretical spin-only value for Mn^{2+} is 5.92 μ_B).

A preliminary structure describing a manganese *N*-pyridoxylidenevaline Schiff base complex has been reported.[25] While no final detailed structure report has appeared, the general features of the Mn(*N*-pyridoxylidenevaline)$_2$ complex conform well to what is observed here. The entire complex also sits on a 2-fold crystallographic axis with a reported Mn–O(phenolate) distance of 2.08 Å (no esd given), which compares favorably with the Mn–O1(phenolate) distance of 2.0907 (8) Å reported in this study for Mn(PLED^{2-}).

The crystal structures of related *N*-pyridoxylideneglycine Schiff base complexes with Ni(II) and Cu(II) have also been reported.[26] The Ni(II) complex is pseudooctahedral, with the same approximate coordination-site geometry and ligand donor atom set described here. The Cu(II) complex is square pyramidal, with basal coordination from the nitrogen and phenolate atoms. Because of the smaller ionic radii of Ni(II) and Cu(II), these metal ions form more stable complexes, with resultant shorter bond distances, than found for the Mn(II) complex reported here.

The bond angles and distances within the PLED ligand are presented in Table III. Five different types of hydrogen bonds are found in the crystal structure of **1**. Of particular interest for MRI applications are the four water molecules next to the manganese atom (Figure 1). Although linked to each other, they are held by hydrogen bonds to O1 and O3 at Mn–O distances of 4.4981 (11) Å (Mn–O5) and 4.4011 (12) Å (Mn–O6).

Potentiometric Measurements. Although seven protonations in the pH range 2–12 were reported by Taliaferro et al.,[3a] the present study revealed only six protonations. It is noted that the log K value of 5.73 assigned to equilibrium [H_5L]/[H_4L][H] in ref 3a is omitted from the subsequent NMR investigation of PLED by Taliaferro and Martell.[3b] Since the results of the present study proved to be reproducible and are within accepted precision limits, metal ion stability constants were determined for PLED with Zn^{2+}, Cu^{2+}, and Mn^{2+} and are shown in Table V.

The potentiometric titration curves for PLED, Mn(PLED^{2-}), and Cu(PLED^{2-}) at 3 mM concentrations are shown in Figure

(21) I, T.-P.; Nancollas, G. H. *Anal. Chem.* **1972**, *44*, 1940–1950.
(22) Evans, D. F. *J. Chem. Soc.* **1959**, 2003–2005.
(23) Shannon, R. D. *Acta Crystallogr., Sect. A: Cryst. Phys., Diffr., Theor. Gen. Crystallogr.* **1976**, *A32*, 751.
(24) Johnson, C. K. Report ORNL-3794; Oak Ridge National Laboratory: Oak Ridge, TN, 1965.
(25) Willstadter, E.; Hamor, T. A.; Hoard, J. L. *J. Am. Chem. Soc.* **1963**, *85*, 1205–1206.
(26) Sudhakara Rao, S. P.; Manohar, H.; Bau, R. *J. Chem. Soc., Dalton Trans.* **1985**, 2051–2057.

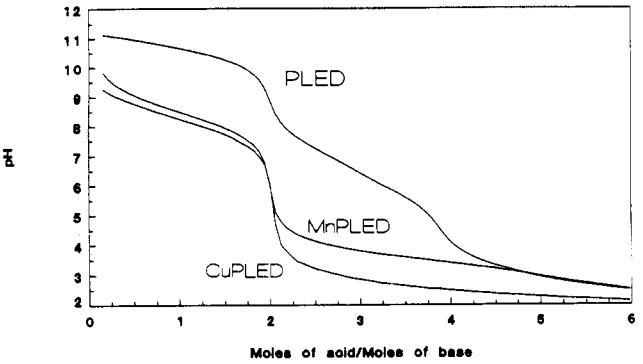

Figure 3. Potentiometric titration curves of PLED in the presence and absence of equimolar Mn^{2+}. Concentrations of the metal ion and ligand are 3.00×10^{-3} M (μ = 0.10 M (NaCl), T = 25 °C).

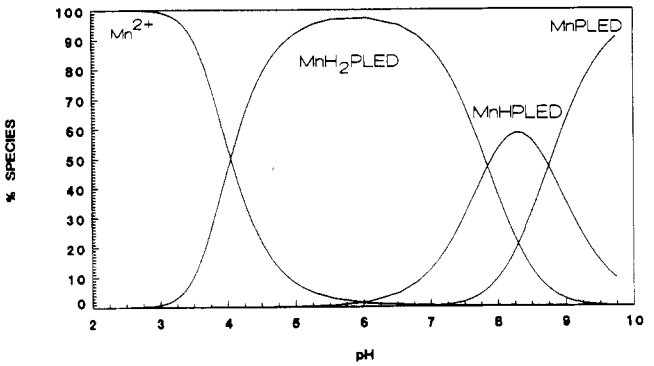

Figure 4. Distribution of species as a function of pH for 1×10^{-3} M $Mn(PLED^{2-})$ (μ = 0.10 M (NaCl), T = 25 °C).

3. The dramatic decrease in pH observed following the addition of 2 equiv of acid represents protonation of the only available protonation sites of the Mn(II) and Cu(II) complexes (the two pyridine nitrogen atoms). Further addition of acid (5 equiv total) leads to complete dissociation of the $Mn(PLED^{2-})$ complex at pH 3. The $Cu(PLED^{2-})$ curve demonstrates the lack of complex dissociation as low as pH 2 and therefore cannot be studied by direct titration methods. The species distribution curves for the protonated forms of $Mn(PLED^{2-})$ are shown in Figure 4.

The stability constant values for $Cu(PLED^{2-})$ were obtained by a competitive ligand/ligand titration of Cu^{2+}, PLED, and EDTA. The thermodynamic stability of $Cu(EDTA^{2-})$ is less than that for $Cu(PLED^{2-})$ by a factor of $10^{2.6}$. In a 1:1:1 solution of Cu^{2+}/PLED/EDTA at a pH high enough to deprotonate both EDTA and PLED, Cu^{2+} is essentially 100% complexed by PLED. However, as the pH of the solution is lowered, the overall more basic PLED ligand ($\sum \log K_H \approx 40$) undergoes greater proton competition than EDTA ($\sum \log K_H \approx 22$), and hence, $Cu(EDTA^{2-})$ becomes more stable by a factor of ca. 2 at pH 2.

The relatively low formation constant of $Mn(PLED^{2-})$ as compared to those of Zn^{2+} and Cu^{2+} is due to the comparatively large size of Mn^{2+} as well as its lack of ligand field stabilization energy (unlike Cu^{2+}). The protonation constants of $Mn(PLED^{2-})$ are only slightly different from those of $Cu(PLED^{2-})$ and $Zn(PLED^{2-})$ despite the large difference in initial complex stability and metal ion size. This is a strong indication that the protonation of these complexes takes place at the uncoordinated nitrogen atoms of the pyridine rings.

Conclusions. This work describes the isolation, structural determination, and determination of thermodynamic equilibrium properties of a hydrolytically stable manganese(II) hexadentate chelate. The crystal structure of $Mn(PLED^{2-})$ shows that (i) the manganese is in the +2 oxidation state and (ii) there are four water molecules in close proximity (4.4–4.5 Å) to the metal center. The possible mechanisms for proton relaxation with $Mn(PLED^{2-})$ include (1) outer-sphere water exchange via the hydrogen-bonding network described by the crystal structure of $Mn(PLED^{2-})$ and (2) proton–proton exchange at the pyridine nitogen atoms. Although the pyridine nitrogens are 5.9 Å from the paramagnetic Mn(II), ring-current effects may lead to enhanced relaxation of these exchangeable protons. The magnitude of the proton relaxivity of $Mn(PLED^{2-})$ has been established by NMR relaxation studies and will be reported elsewhere.

The solution equilibrium studies demonstrate the relatively high affinity of PLED for manganese(II), although $Mn(PLED^{2-})$ has a stability constant less than $Mn(EDTA^{2-})$. $Mn(PLED^{2-})$ can coordinate two protons at neutral pH without dissociation of the complex. The basicity of the aliphatic nitrogens, phenolates, and carboxylates of PLED ($\sum \log K_H \approx 25$) is slightly higher than the overall basicity of EDTA ($\sum \log K_H \approx 22$). These ligand basicities would predict a higher stability constant for $Mn(PLED^{2-})$ than for $Mn(EDTA^{2-})$. However, this study has determined the stability constant of $Mn(PLED^{2-})$ ($\log K = 12.56$) to be less than that of $Mn(EDTA^{2-})$ ($\log K = 13.95$). These results may be explained by considering the steric repulsions of the substituted pyridine groups as well as the size requirement of the six-membered phenolate–aliphatic nitrogen chelate ring.

Supplementary Material Available: Table SI (a detailed list of the crystallographic data collection parameters), Table SII (least-squares-plane parameters), Table SIII (general temperature factor expressions), and Table SIV (root-mean-square amplitudes of thermal vibration) (5 pages); Table SV (values of calculated and observed structure factor amplitudes) (10 pages). Ordering information is given on any current masthead page.